9 Tumor Imaging with Special Emphasis on the Role of Positron Emission Tomography in Radiation Treatment Planning

Anca-Ligia Grosu, Wolfgang A. Weber, and Ursula Nestle

CONTENTS

KEY POINTS

- Radiological imaging of malignant processes has evolved tremendously over recent decades. It not only provides better detection with superior anatomical resolution through rapid advances in CT and MRI technology, but it also provides functional and physiological information. For example, in lung cancer the diagnostic accuracy of FDG-PET is between 85% and 90%.
- In brain tumors, the sensitivity and specificity of MET-PET for tumor detection and tumor tissue extension are significantly higher in comparison to MRI, CT or FDG-PET.
- While CT-based three-dimensional (3-D) treatment planning already represented a major step compared to the 2-D era, integration of MRI and PET and refinement of image fusion techniques resulted in further significant improvements.
- The high percentage of changes in radiotherapy target volumes of lung cancer patients by FDG-PET reported in the literature is mainly caused by two factors: the ability to distinguish the tumor from collapsed lung tissue and the higher accuracy of FDG-PET in lymph node staging compared to CT.
- Problems include the low resolution of PET images, which is caused by physical factors (size of the detector crystals, positron range in matter, non-collinearity of annihilation gamma rays and detector scatter) and also by movement of the target during acquisition due to relatively long acquisition times, which leads to a blurred margin of the accumulating structure. Other problems include patient positioning and image coregistration.

A.-L. Grosu, MD
Department of Radiation Oncology, Universitätsklinikum Freiburg, Robert-Koch-Straße 3, 79106 Freiburg, Germany
W. A. Weber, MD
Department of Nuclear Medicine, Universitätsklinikum Freiburg, Robert-Koch-Straße 3, 79106 Freiburg, Germany
U. Nestle, MD
Department of Radiation Oncology, Universitätsklinikum Freiburg, Robert-Koch-Straße 3, 79106 Freiburg, Germany

- The possible impact of FDG-PET for target volume delineation in head and neck cancer has been investigated in several trials. All these studies showed that FDG-PET could have a significant impact on gross target volume (GTV) delineation in comparison to CT (or MRI) alone. Here, as in lung tumors, in about one third of cases FDG-PET led to an increase in GTV, whereas in another one third of cases the GTV became smaller, if based on FDG alone.
- In recent years, PET tracers have been developed that can visualize biological pathways with particular significance for tumor response to the treatment. These are, for example, hypoxia, cell proliferation, and angiogenesis.
- Ongoing clinical studies will provide important data on the added value of PET, dynamic MRI, diffusion tensor MRI, and other recently developed imaging methods regarding target volume delineation as well as response monitoring.

Abstract

Precise imaging of the primary tumor, the drainage lymph nodes, and possible sites of distant metastases is mandatory to stage a malignant disease, arrive at a treatment recommendation, and eventually define an accurate gross tumor and clinical target volume for radiotherapy. Better target definition and delineation on a daily basis is surely important in quality assurance for fractionated radiation therapy. The availability of metabolic images obtained by magnetic resonance (MR) spectroscopy, positron emission tomography (PET), and others impacts on staging, treatment planning, and response monitoring. A broad range of techniques, including dynamic magnetic resonance imaging (MRI), PET, and single-photon emission computed tomography (SPECT), provide measurements of various features of tumor blood flow and microvasculature. Using PET to measure glucose consumption enables visualization of tumor metabolism, and MR spectroscopy techniques provide complementary information on energy metabolism. Changes in protein and DNA synthesis can be assessed through uptake of labeled amino acids and nucleosides. Advanced imaging techniques can be used to assess tumor malignancy, extent, and infiltration, and might provide diagnostic clues to distinguish between lesion types. For the detection of metastatic lymph nodes, lymphotropic nanoparticle-enhanced MRI using ultra-small superparamagnetic iron oxide particles has greater accuracy as compared with conventional techniques and has been instrumental in delineating the lymphatic drainage of the prostate gland. The focus of the present chapter is the impact of PET on radiation treatment planning.

9.1 Introduction

The first rationale for using positron emission tomography (PET) in target volume delineation for radiation treatment planning is the higher sensitivity and specificity of PET for tumor tissue, in comparison to computed tomography (CT) and magnetic resonance imaging (MRI), in some tumor entities. This has been demonstrated in many studies that compared the results of PET with the results of the radiological investigations and histology. The hypothesis tested in these studies was that using PET in addition to CT and/or MRI enables tumor tissue detection with a higher accuracy. The ideal PET tracer in this situation should be taken up homogenously from all the cells of the whole tumor and the intensity of the PET uptake should be directly proportional to the density of tumor cells.

The second rationale for integrating PET in the process of radiation treatment planning is the ability of PET to visualize biological pathways, which can be targeted by radiation therapy. The imaging of hypoxia, angiogenesis, proliferation, apoptosis, etc. leads to the identification of different areas within an inhomogeneous tumor mass, areas which can be individually targeted. For example, hypoxic areas can be treated with higher radiation doses than non-hypoxic areas.

The goal of this chapter is to discuss the use of PET for target delineation in the process of radiation treatment planning.

9.2 PET for Target Volume Delineation

The impact of PET for gross tumor volume (GTV) delineation will be discussed based on three examples: amino acids-PET in brain gliomas, fluorine-18-labeled glucose analog fluorodeoxyglucose (FDG)-PET in lung cancer, and FDG-PET in head and neck tumors.

9.2.1 Amino Acids-PET and Single-Photon Emission CT in Brain Tumors

^{11}C-labeled methionine (MET), ^{123}I-labeled alpha-methyltyrosine (IMT), and ^{18}F-labeled O-(2-fluoroethyl)-L-tyrosine (FET) are the most important radiolabeled amino acids used in the diagnosis of brain tumors. These three tracers have shown a very similar uptake intensity and distribution in brain tumors (Langen et al. 1997; Weber et al. 2000). Currently available amino acid-PET tracers are accumulated by L and A amino acid transporters. Tumor cells take up radiolabeled amino acids at a high rate, while there is only a relatively low uptake in normal cerebral tissue. At the level of the blood–brain barrier (BBB) they are independent from the BBB disturbance.

Summarizing the data of the literature based on a PubMed search (using the key words: methionine, PET, and brain tumors) we found 45 clinical trials published between 1983 and March 2007, including 1,721 patients. In 11 studies investigating 706 patients, the data were analyzed using MET-PET-guided stereotactic biopsies. The main message of the trials is that the sensitivity and the specificity of MET-PET for tumor detection and tumor tissue extension are significantly higher in comparison to MRI, CT, or FDG-PET (Weber et al. 2008).

We evaluated the impact of MET-PET in target volume delineation for radiation treatment planning, compared to MRI, in 39 patients with brain gliomas after tumor resection (Grosu et al. 2003, 2005a). MET uptake corresponded to the gadolinium (Gd) enhancement in only 13% of the cases. In 74% of the patients MET volume extended beyond the contrast-enhancing regions, indicating residual tumor. In 69% of the cases Gd enhancement could be outlined beyond the volume of MET uptake, showing postoperative BBB disturbance. Similar results were also reported evaluating the impact of IMT-single-photon emission CT (SPECT) in target volume delineation in non-resected (Grosu et al. 2000) and resected (Grosu et al. 2002) patients with gliomas. Focal IMT uptake after tumor resection was highly correlated with poor survival, suggesting that amino acids are specific markers for residual tumor tissue (Weber et al. 2001). The first study evaluating the value of MET-PET or IMT-SPECT for treatment outcome was performed in 44 patients with recurrent gliomas re-irradiated using stereotactic fractionated radiotherapy (SFR) (Grosu et al. 2005b). A prospective non-randomized trial has shown that in patients treated based on amino acids-PET or -SPECT, the median survival time was significant higher (9 months) in comparison to patients treated based on CT/MRI alone (5 months, p=0.03). The results of this pilot study have yet to be verified in a randomized trial.

9.2.2 FDG-PET in Gross Tumor Volume Delineation of Lung Cancer

In lung cancer, the diagnostic accuracy of FDG-PET is between 85% and 90% (Figs. 9.1, 9.2) (Dwamena et al. 1999; Hellwig et al. 2001; MacManus et al. 2001). In the late 1990s this promising diagnostic performance led to the idea of integrating PET into radiotherapy planning (Munley et al. 1999; Nestle et al. 1999).

In earlier reviews (Grosu et al. 2005c; Nestle et al. 2002, 2006) the literature about the integration of FDG-PET in radiotherapy planning of non-small cell lung cancer (NSCLC) has been surveyed. To date, over 20 studies in more than 600 patients have shown that the use of FDG-PET image data may lead to an advantage for the patient. The main sources of this possible advantage are the better coverage of the primary tumor and the protection of healthy tissue. In this context it is interesting that the FDG-based target volumes may be both smaller or larger compared to CT-based ones. The high percentage of changes in target volumes by FDG-PET (20–100%) reported in the literature concerning various parameters of the planning process (field sizes, GTV, clinical target volume [CTV], planning target volume [PTV], normal tissue complication probability [NTCP], etc.) is mainly caused by two factors: the ability to distinguish the tumor from collapsed lung tissue (atelectasis) and the higher accuracy of FDG-PET in lymph node staging compared to CT. However, because inflammation in the collapsed lung may also lead to FDG accumulation, PET does not help with GTV definition in these cases.

A significant parameter, especially in the context of collapsed lung tissue, is the reduction of interobserver variability (IOV) of the GTV delineation by FDG data integrated in the planning process. Here, several authors have shown clear improvements (Caldwell et al. 2001; Steenbakkers et al. 2006; Van de Steene et al. 2002). The Toronto group (Caldwell et al. 2001) demonstrated a reduction of the IOV from 1:2.3 to 1:1.6 after adding FDG-PET information to CT images for GTV delineation of advanced NSCLC.

However, despite the improvement of the IOV, the gold standard method for the delineation of the GTV has not been set yet. The problem is the low resolution of PET images, which is caused by physical factors (size of the detector crystals, positron range in matter, non-

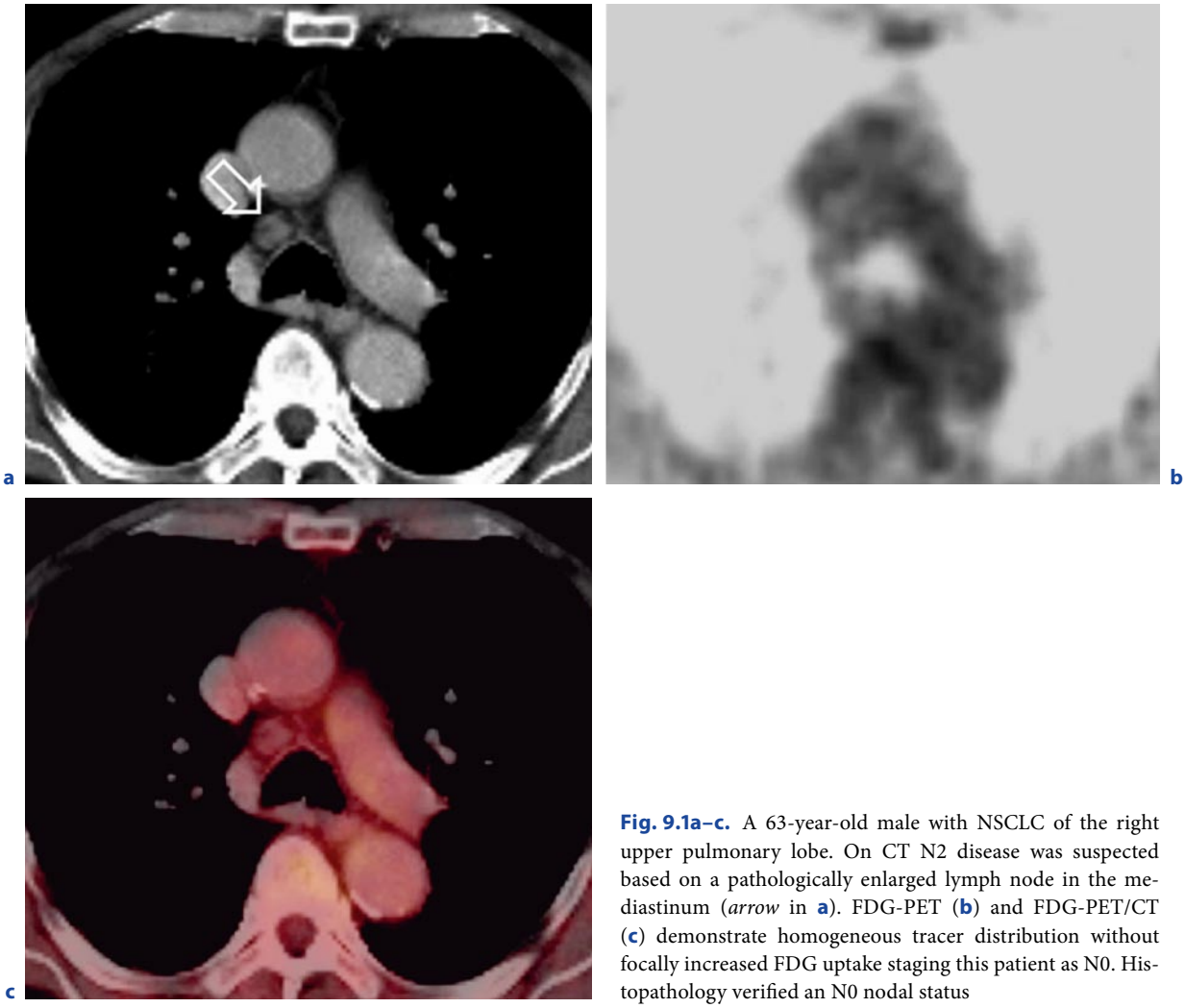

Fig. 9.1a–c. A 63-year-old male with NSCLC of the right upper pulmonary lobe. On CT N2 disease was suspected based on a pathologically enlarged lymph node in the mediastinum (*arrow* in **a**). FDG-PET (**b**) and FDG-PET/CT (**c**) demonstrate homogeneous tracer distribution without focally increased FDG uptake staging this patient as N0. Histopathology verified an N0 nodal status

collinearity of annihilation gamma rays, and detector scatter) (Cherry 2006), and also by biological factors (movements of the target during acquisition due to relatively long acquisition times), which leads to a blurred margin of the accumulating structure (Nestle et al. 2006).

Various methods are used for the delineation of FDG accumulations for GTV contouring. Easily applicable is the visual contouring by the physician, in analogy to the method used with CT-based contouring. However, a significant IOV remains (Pötzsch et al. 2006). To improve this IOV, clinical protocols have been applied (MacManus et al. 2007) and have succeeded in a significant convergence of FDG-based GTVs contoured by different observers. However, visual contouring remains observer dependent and by further distribution of the method into clinical practice, the varying experience of the radiotherapist with PET will influence the quality of visual GTV contouring. Therefore other methods for automatic and/or semiautomatic threshold contouring of the—often high contrast—FDG accumulations have been reported. Easily applicable at most PET and/or radiotherapy planning systems is the use of a threshold of a fixed FDG concentration, expressed as standardized uptake value (SUV, i.e., decay-corrected tissue activity/tissue volume divided by injected activity/body weight). However, there are numerous technical and biological factors influencing the SUV. Furthermore, the FDG accumulation in normal tissues may vary, being even higher than the threshold values suggested in the literature (e.g., SUV=2.5). Therefore, other than for diagnostic purposes where the maximum SUV of a lesion may give an impression of the malignancy of the lesion, the use of a fixed SUV threshold is not suitable for GTV contouring. Also easily applicable at most systems is a threshold relative to

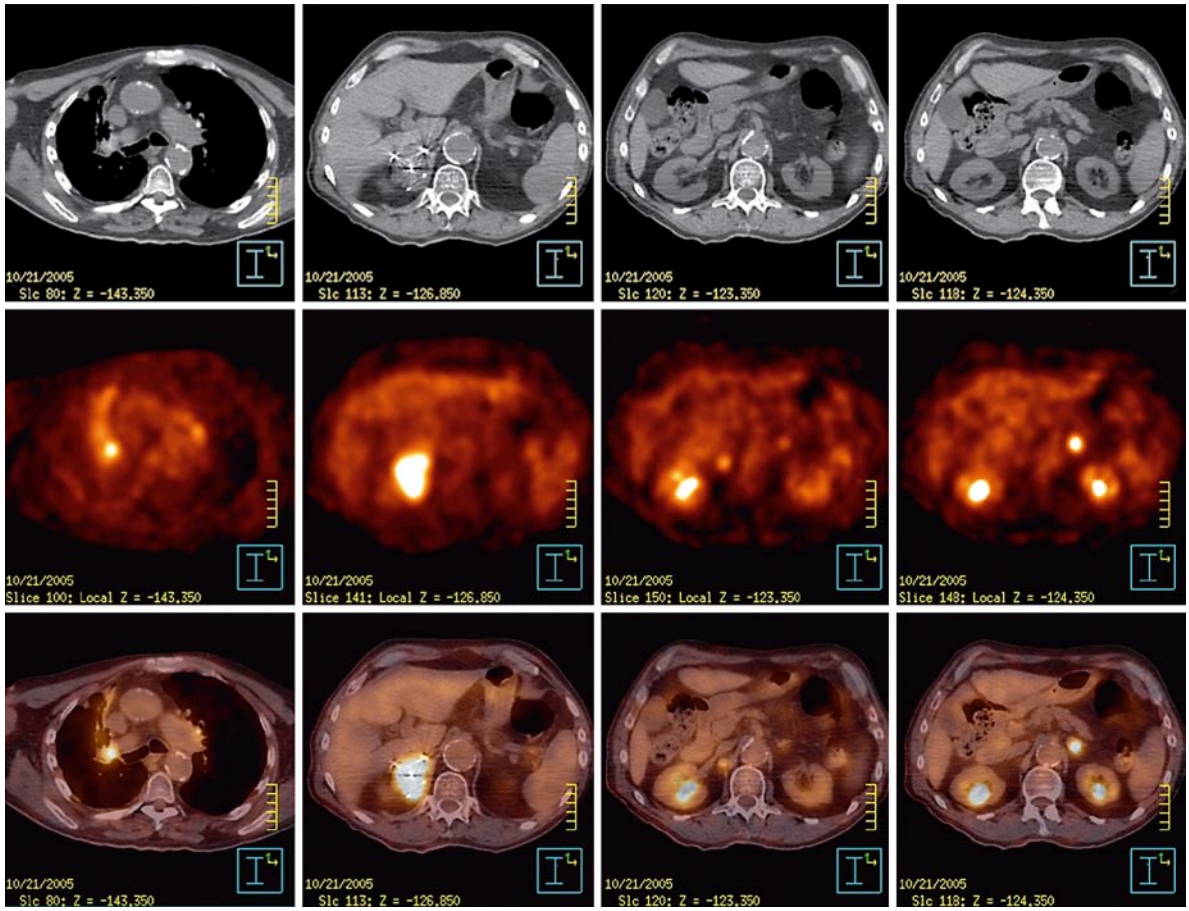

Fig. 9.2. These images are from a 70-year-old male with recurrent small-cell lung cancer evaluated for CyberKnife treatment of an isolated right adrenal lesion. PET/CT showed previously unsuspected mediastinal, left adrenal, and retroperitoneal disease

the maximum FDG accumulation of the lesion. This method is derived from the imaging of homogenous structures such as phantoms filled with radioactivity. In 1997, Erdi et al. used 40% of the maximum FDG accumulation for contouring 17 homogenous lung metastases leading to volumes that were comparable to those measured by CT. Thus, many groups have used this method since then. Meanwhile, it has been shown that ungated PET images may depict the probability of the presence of lung tumors over the whole breathing cycle (Caldwell et al. 2003; Yaremko et al. 2005), which means that the "true" volume of a lung lesion contoured in an FDG-PET dataset must be by the amount of breathing excursions larger than the volume measured in CT. Furthermore, lung tumors often show a relatively inhomogeneous FDG accumulation. Therefore, it has been shown that applied in primary lung tumors, thresholding by a percentage of the maximum accumulation intensity may lead to insufficient coverage of lesions (Nestle et al. 2005).

More promising is the use of contrast-dependent methods (Schaefer et al. 2008). These methods use the information on the accumulation intensity in the questionable lesion as well as in the neighboring background. An example of a relatively simple contrast-oriented method is the "Homburg algorithm" (Schaefer et al. 2008; Nestle et al. 2005, 2007):

$$I_{threshold} = A \times I_{lesion} + B \times I_{background}$$

Here, I_{lesion} is the mean FDG accumulation (SUV or Intensity) of a 3-D isocontour of, for example, 70% of the maximum of the lesion, while $I_{background}$ is the mean FDG accumulation in the surrounding normal tissue. A and B are parameters that mainly depend on the imaging characteristics of the PET system, which has to

be determined by phantom measurements (Schaefer et al. 2008). Other contrast-oriented algorithms lead to similar contouring results and also need a calibration by phantom measurements.

In our experience, other than absolute or relative SUVs, contrast-oriented algorithms are quite robust under clinical conditions. However, the calibration to the PET and radiotherapy planning system used is mandatory (Nestle et al. 2005, 2006, 2007). As technical factors like the methods of reconstruction, attenuation correction of PET images, and data transfer do influence PET imaging, they have to be defined before and kept constant after calibration.

Overall, it must be kept in mind that the choice of the method for GTV contouring may have a significant impact on the size of the GTV (Nestle et al. 2005) and that the most important factor in PET-based GTV delineation is the close collaboration of nuclear medicine and radiotherapy departments on the side of the medical as well as on the side of the physical and technical staff.

Crucial points in this context are patient positioning and image coregistration. It must be kept in mind that patient position may change, not only between acquisition on stand-alone PET and CT scanners, but also during PET/CT acquisition. Not correcting for the consequent differences in tumor localization leads to a geographical miss, if PET-derived GTVs are transmitted to CT datasets without critical evaluation of the quality of coregistration. This is best done by comparing anatomical landmarks detectable by both imaging techniques, such as carina tracheae, lung apices, spine, sternum, thoracic wall, and—with care due to breathing mobility—diaphragm. Although non-rigid coregistration algorithms may solve some of the positioning problems, at the moment, rigid coregistration algorithms are the method of choice. It may well be that the deformation of the image data caused by non-rigid algorithms may result in geometrical inexactnesses or geographical misses, especially in tumors which are not clearly depicted by the morphological method. Unfortunately, these are the cases in which the integration of FDG-PET into radiotherapy planning is most helpful. Further research is needed to clarify this point.

The highest possible benefit for the patients from FDG-based radiotherapy planning can only be gained if, due to the exact depiction of tumor localization by PET, the irradiation of normal tissues can be omitted. In lung cancer, this would mean departing from the clinical concept of "elective nodal irradiation" (ENI) of large macroscopically normal parts of the mediastinum when defining the CTV (Kiricuta 2001). Omitting ENI could lead to a significant protection of highly radiosensitive normal tissues, for example lung, with the consequence of obtaining higher irradiation doses in the tumor. First clinical data with (De Ruysscher et al. 2005) and even without FDG-PET (Rosenzweig et al. 2007) have shown that the risk of "out of field" recurrences after targeting the macroscopic tumor alone is small, much smaller than the risk for local ("in field") tumor progression. However, prospective randomized clinical studies will have to show that this policy is safe and beneficial for the patients. The data from 26 patients with NSCLC treated with involved-field radiotherapy who had local failure and a post-radiotherapy PET scan were analyzed by Sura et al. (2008). The patterns of failure were visually scored and defined as follows: (1) within the GTV/PTV; (2) within the GTV, PTV, and outward; (3) within the PTV and outward; and (4) outside the PTV. Local failure was also evaluated as originating from nodal areas versus the primary tumor. All the patients had recurrence originating from their primary tumor. Of 8 primary tumors that had received a dose of <60 Gy, 6 (75%) had failure within the GTV and 2 (25%) at the GTV margin. At doses of ≥60 Gy,

▸ **Fig. 9.3a–d.** Central necrosis of metastatic lymph nodes. **a,b** Bilateral nodal metastases of oropharyngeal SCC. **a** Post-contrast CSE T1-weighted coronal image with FS shows three different metastatic nodal patterns: (1) an area of low signal intensity surrounded by an intensely contrast-enhanced rim (*black curved arrow*); (2) an area of intermediate signal intensity with a bright rim (*thin white arrow*); (3) an area of intermediate signal intensity partially "obscured" by an intensely "flashing" rim (*thick white arrow*). Fat is well suppressed at the level of the white star, but less satisfactorily so at the level of the white notch. **b** FSE T2-weighted coronal image without FS in a strictly similar slice location to 3a clearly reveals central necrosis as a very bright cystic area within the node displaying the lowest T1 signal intensity (*black curved arrow*), whereas the other nodes are not necrotic-cystic. **c,d** Close-ups of metastatic jugular nodes of an infiltrating SCC of the right vallecula (*white notch*). **c** Post-contrast CSE transverse T1-weighted image without FS. Necrotic areas within the nodes display very low signal intensity (*arrowheads*). A non-necrotic lymph node (*arrow*) and submandibular gland (*double arrows*) exhibit similar signal intensity. **d** FSE T2-weighted transverse image without FS in a similar slice location to that in 3c shows very bright signal intensity of the nodal necrotic-cystic areas. Signal intensities of the non-necrotic node and the submandibular gland are significantly different

6 (33%) of 18 had failure within the GTV, 11 (61%) at the GTV margin, and 1 (6%) was a marginal miss ($p<0.05$). The authors concluded that with lower doses, the pattern of recurrences was mostly within the GTV, suggesting that the dose might have been a factor for tumor control, whereas at greater doses, the treatment failures were mostly at the margin of the GTV. They also mentioned that visual incorporation of PET data for GTV delineation might be inadequate, and more sophisticated approaches of PET registration should be evaluated.

9.2.3 FDG-PET in Head and Neck Cancer

Anatomical imaging continues to provide important information on disease extent and prognostic factors, as illustrated in Fig. 9.3. However, other imaging methods are being used in addition to CT and MRI. Gambhir et al. (2001) summarized the data of eight studies (468 patients) that evaluated the impact of FDG-PET in staging of head and neck cancer: the average sensitivity and specificity for FDG-PET were 87% and 89%, respectively, whereas for CT were 62% and 73%, respectively. For tumor diagnosis the sensitivity and specificity of FDG-PET, assessed in seven trials incorporating 193 patient studies, were 93% and 70%, in comparison to CT with 66% and 56%, respectively. However, the standard diagnosis of tumor infiltration in head and neck cancer remains the histological evaluation.

Since this analysis was published, more advanced data have been reported: Liu et al. (2007) performed a systematic review of the performance of FDG-PET in head and neck cancer, namely about diagnosis of residual or recurrent nasopharyngeal carcinoma. In this thoroughly conducted analysis of data from 1,813 patients, FDG-PET compared to CT and MRI is by far the method with the best diagnostic performance: the overall sensitivity of PET being 0.95 and 0.9 versus 0.76 and 0.59 for CT and 0.78 and 0.76 for MRI.

Furthermore, the new technology of combined PET/CT has been brought into the clinic and was evaluated by several groups. Hybrid PET/CT enables a better correlation of FDG accumulations with anatomy, which is very helpful for the interpretation of PET scans in the topographically complex head and neck region. Overall, it has been shown that the diagnostic accuracy of PET/CT, especially concerning equivocal findings, is higher compared to that of PET alone (Jeong et al. 2002) and maintains the superiority of FDG-PET compared to CT (Schwartz et al. 2005a) and to MRI (Dresel et al. 2003).

However, as in lung cancer, the diagnostic accuracy of FDG-PET and/or PET/CT in head and neck cancer is not 100%. The main causes for false-negative findings are again the presence of micrometastatic disease in lymph nodes or very small primary lesions. False-negative PET results may also be caused by flat superficial growth, which is not uncommon in this area (Dresel et al. 2003). In a group of 116 patients with mixed stage and site primary or recurrent head and neck tumors, Dresel et al. (2003) diagnosed 86% of the tumors and 82% of the involved cervical lymph nodes correctly, translating to false-negative rates of 14–18%. In a highly preselected group of operated clinically N0 patients with oral cancer, with 9/142 histologically metastatic lymph node levels, Schöder et al. (2006) described 3/9 false FDG-negative lymph node levels (1 directly adjacent to the primary tumor). Therefore, the rates of false-negative FDG-PET findings in head and neck patients seem to be higher than in lung cancer, although no meta-analysis on this topic has been performed yet. For the surgical treatment, however, it has been concluded that management of cervical lymph nodes should not be based on FDG-PET/CT alone.

False-positive FDG-PET findings, as was also seen in the Schöder group of patients and in many other diagnostic studies (Chan et al. 2006; Dresel et al. 2003; Goshen et al. 2006), may be caused by inflammation accounting for 6/133 false FDG-positive neck levels caused by inflammatory lymphoid hyperplasia in the Schöder data. False-positive FDG accumulations may furthermore be found in the metabolically active lymphoid tissues of the tonsils, the base of tongue, and the Waldeyer's ring, while a variable symmetric or asymmetric uptake may be seen in salivary glands and may also be variable in muscles, including the larynx, depending on the activities of the patient after injection of the FDG (Abouzied et al. 2005). By including the anatomical information of CT (Nakamoto et al. 2005), the rates of false-positive FDG-PET/CT findings appear lower than those reported in the earlier literature on FDG-PET alone (Goshen et al. 2006; Zimny et al. 2002).

There are two main technical problems in FDG-based definition of target volumes for patients with head and neck cancer: coregistration and GTV delineation:

1. Coregistration is a delicate problem in the head and neck area. Impreciseness in coregistration of some millimeters may soon lead to a significant geographical miss in the complex flexible anatomy with the structures of interest being relatively small. When using rigid coregistration algorithms, positioning aids like masks used for radiotherapy must be used for the PET acquisition, too. If these are not used, PET scans from this area of the body can not be rigidly registered to a planning CT or MRI with sufficient accuracy. Although non-rigid coregistration algorithms are advocated by some authors (Ireland et al. 2007) to solve the positioning problem, it has not yet been proven that with non-rigid coregistration of image data the tumor structures are registered correctly to anatomical imaging. To our knowledge there is no method available to date that can take into account, for example, the different grades of rigidity of anatomical structures (e.g. bone, soft tissue, airways, etc.) in the head and neck area. Therefore, further research is needed at this point. Until then, thorough patient positioning for

PET, CT, and treatment application and rigid image coregistration is mandatory.

2. FDG-based delineation of the GTV is another challenging problem. The key feature in this context is that the structures of interest are relatively small compared to a voxel size of PET. Including one set of surrounding voxels more or less into the GTV may lead to significant changes of volume, and therefore of tumor covering on one side and normal tissue complications on the other side. As had been seen by Ford et al. (2006), who compared different percentages of the maximum intensity as thresholds, the Nijmegen group (Schinagl et al. 2007) also showed large differences in the resulting volumes between various methods applied for GTV contouring, which led to differences of nearly 100%. The Nijmegen group concluded that, as in lung cancer, a contrast-oriented method (source/background ratio) seems preferable. The Ghent group (Daisne et al. 2003, 2004) showed that by contouring larynx cancers preoperatively by a contrast-oriented method the results in comparison to pathological specimens were more accurate than CT- and MRI-based GTV delineation. However, in a later planning trial on intensity-modulated radiotherapy (IMRT), the same group (Geets et al. 2007) favored another, gradient-based method.

In a first clinical trial with 41 patients, the group of Madani et al. (2007) performed an FDG-guided focal dose escalation using IMRT for patients with head and neck cancer. While applying conservative doses to elective lymph node levels, doses to GTVs defined by CT and FDG-PET were escalated up to a NID_{2Gy} of 78.2 Gy. However, in preliminary evaluation of the pattern of recurrence, 4/9 locoregional recurrences were located outside the PET-defined GTV and 1/9 at the border of the PET-defined GTV, although the above-mentioned contrast-oriented method for FDG-based GTV contouring was used, which had been verified by correlation with pathological specimens (Daisne et al. 2004). Possible reasons for the relatively high rate of recurrences outside the PET-defined GTV are false FDG-negative nodal disease together with steep dose gradients in the IMRT plans and the fact that not all patients received concomitant chemotherapy. However, the other 4/9 locoregional recurrences appeared within the high-dose volumes showing the need for further dose escalation to the gross tumor while 9/14 relapsing patients had distant metastases, supporting the need for additional chemotherapy.

The possible impact of FDG-PET for target volume delineation for radiation treatment planning has meanwhile been investigated in nine trials (Ciernik et al. 2003; Connell et al. 2007; Daisne et al. 2004; Geets et al. 2007; Nishioka et al. 2002; Paulino et al. 2005; Rahn et al. 1998; Scarfone et al. 2004; Schwartz et al. 2005b) incorporating 248 patients with different tumor stages and locations. All these studies showed that FDG-PET could have a significant impact on GTV delineation in comparison to CT (or MRI) alone, the results ranging between 9% and 100% of the cases. Here, as in lung tumors, in each about one third of cases FDG-PET led to an increase of GTV, whereas in another one third of cases the GTV became smaller, if based on FDG alone. Therefore, an FDG-based radiotherapy of head and neck cancer patients might lead to a significant gain in normal tissue protection especially concerning the parotid gland, with a relevant improvement of quality of life.

Overall, the optimum method for GTV delineation in this area has not been defined yet. In the end, the results of further clinical trials will have to show if it is beneficial to use FDG-PET-based GTV reduction in the radiotherapy planning of head and neck tumors.

9.3 PET for Visualization of Tumor Biology

In recent years, PET tracers have been developed that can visualize biological pathways with particular significance for tumor response to the treatment. These are, for example, hypoxia, cell proliferation, and angiogenesis. The volumes defined by using images acquired after injection of these tracers may be used as subvolumes of the tumor, like a target within the GTV, which could be irradiated with a higher dose, for example by IMRT. This concept is called "dose painting," and is as yet a promising hypothesis waiting to be validated by clinical and experimental data (Bentzen 2005; Bradley et al. 2004; Buck et al. 2005; Ling et al. 2000, 2004; Tanderup et al. 2006).

9.3.1 Hypoxia

Hypoxia, i.e., an insufficient tissue oxygenation, is a well-known factor causing radioresistance of cells. Clinically, low tumor oxygenation, for example in patients with head and neck tumors, has been shown to be associated with a poor prognosis after radiotherapy (Nordsmark et al. 2005). Although the underlying mechanisms of radioresistance are still subject to inves-

tigation (Koritzinsky et al. 2005; Troost et al. 2005; Williams et al. 2005; Yaromina et al. 2005), it appears very interesting to image hypoxia in vivo in order to increase local doses to radioresistant regions. Several bioreductive substances have been evaluated as hypoxia tracers. The tracers investigated are mainly nitroimidazole compounds, for example [^{18}F]-fluoromisonidazole ([^{18}F]-FMISO), which was the first nitroimidazole compound developed for PET, [^{123}I]-iodoazomycin arabinoside ([^{123}I]-IAZA) and [^{18}F]-azomycin arabinoside ([^{18}F]-FAZA). With these tracers, the bioreductive molecule attracts a single electron leading to free radical metabolites that are further reduced and bound to cell constituents under hypoxic conditions. [^{60}Cu]-labeled methylthiosemicarbazone ([^{60}Cu]-ATSM) has also being proposed for hypoxia imaging.

The first data about the use of hypoxia PET for the visualization of a hypoxic subvolume were published by a group at the University of Washington (Koh et al. 1995; Rasey et al. 1996). Based on experimental and clinical data, they considered a tumor pixel with a tumor/blood [^{18}F]-FMISO ratio ≥1.4 at the late image acquisition interval (120 min following injection) as indicative for the presence of hypoxia. Therefore, the percentage of pixels within the imaged volume that had a tumor/blood [^{18}F]-FMISO ratio ≥1.4 were defined as fractional hypoxic volume (FHV). The authors assessed the dynamics of FHV during radiotherapy in 7 patients with NSCLC and showed that it decreased from the beginning to the end of the treatment (Koh et al. 1995). In a study published about 10 years later, the Tübingen group assessed the predictive value of [^{18}F]-FMISO after radiation therapy in 14 patients with NSCLC and 26 patients with head and neck cancer (Eschmann et al. 2005). In the lung cancer group SUV measured 4 h after tracer injection did not correlate with the tumor recurrence after radiotherapy, whereas in the head and neck group for an SUV >2 the correlation was statistically significant. A tumor-to-mediastinum ratio >2 was a predictive factor for local recurrence in the lung cancer group. The authors performed qualitative analysis of time–activity curves and defined three curve types: rapid tracer washout, intermediate (delayed) washout, and a tracer accumulation curve. The tracer accumulation curve correlated with a higher incidence of local recurrence, while the rapid-washout curve was a predictive factor for better local tumor control.

[^{60}Cu]-ATSM is a bioreductive molecule also being proposed for tumor hypoxia imaging. In a trial including 14 patients with NSCLC treated with radiation and/or chemotherapy it was shown that the mean tumor-to-muscle activity ratio before treatment was significantly lower in responders (1.5±0.4) than in non-responders (3.4±0.8; p=0.002). The tumor/muscle ratio of 3 could discriminate the responders from non-responders. The mean SUV for [^{60}Cu]-ATSM was not significantly different in responders versus non-responders (Dehdashti et al. 2003). Grosu et al. (2007) evaluated the distribution of hypoxia in 18 patients with head and neck tumors using FAZA-PET. The hypoxic subvolume was located in a single confluent area in 61% of patients, was diffusely dispersed in the whole tumor mass in 22%, and missing in 17%. Only patients with a confluent distribution of the tracer would be suitable for a dose painting approach based on hypoxia. However, such an approach could lead to a dose escalation to 105 Gy in tumor without exceeding the normal tissue tolerance (Lee et al. 2008).

The results of these studies could open new perspectives for radiation treatment planning. They demonstrated the feasibility of in vivo PET studies performed with tracers which in experimental models were closely related to tissue hypoxia. Furthermore, they showed, even in a small number of patients, a significant correlation between hypoxia-tracer uptake and treatment response. However, clinical trials analyzing the impact of FHV as a target for radiation treatment planning in lung cancer have not been done so far.

In the preparation of such trials, several issues have to be addressed. Firstly, the tracer used for radiotherapy application must be carefully chosen. It would ideally be captured specifically by hypoxic cells using an oxygen-specific retention mechanism, be sufficiently delivered in a perfusion-limited microenvironment, produce a low level of non-specific metabolites, and have no labeled metabolites of hypoxia tracers found in the circulation at the time of imaging. Secondly, the method of quantification must be sorted out. Considering the phenomena of perfusion, diffusion, and hypoxia-induced tracer retention and inspired by recent immunohistochemical investigations with the hypoxia tracer pimonidazole (Bussink et al. 2003), the Tübingen group proposed that the kinetic model is a more valid criterion to quantify hypoxia in vivo than a criterion based on static SUV at an early time point. However, depending on the tracer used, static imaging, which is much easier to implement in the planning process, may also be feasible. Thirdly, the method of application of radiotherapy must be chosen. To date, two IMRT models are proposed: The model of Chao et al. (2001) is defined as a target in target, which by using IMRT is irradiated with a higher dose than the rest of the tumor. In a more sophisticated technique, Alber et al. (2003) propose a method which allows the inclusion of biological imaging data in the

optimization of IMRT to produce an image intensity based dose modulation, voxel by voxel.

An essential question, however, is how to account for setup variations and target movements. Due to the relatively low contrast of hypoxia-PET images, contouring hypoxia targets can be expected to pose more problems than [^{18}F]-FDG imaging already does. Furthermore, setup and target movement errors have to be applied when using these data for PTV delineation. Depending on the quality of immobilization, it may be necessary to apply margins to every voxel of the GTV with a defined dose prescription.

Another essential question addresses the reproducibility of the intratumoral distribution of hypoxia. In a recent study Nehmeh et al. (2008) evaluated the dynamics of the FMISO uptake in PET over 3 days in 14 patients with untreated head and neck tumors. The authors describe variability in spatial hypoxia tracer uptake. Only 6/13 patients had well-correlated intratumoral distributions of FMISO, suggestive of chronic hypoxia.

In the end, the results of such clinical trials will have to be awaited to find out about the clinical benefit from hypoxia-based dose intensification.

9.3.2 Proliferation

The proliferation of tumor cells is the basic mechanism for malignant growth. Therefore, it has been tried to image this parameter, which is thought to be more specific for malignancy compared to, for example, glucose consumption. [^{18}F]-fluorine-labeled thymidine analog 3'-deoxy-3'-[^{18}F]-fluorothymidine (FLT) is retained in the cell after phosphorylation by thymidine kinase 1, whose levels correlate with cell proliferation.

The FLT uptake in malignant tissue, measured by SUV, seems to be generally lower than the [^{18}F]-FDG uptake. The sensitivity seems to be higher for primary tumors than for lymph node metastases (Buck et al. 2005). Furthermore, the specificity of the tracer is not 100%: proliferation of lymphocytes and non-specific increased accumulation due to increased perfusion and vascular permeability could lead to false-positive results (Shields et al. 1998; Yap et al. 2006).

Until now, there are no trials analyzing the impact of FLT-PET on radiation treatment planning. However, it visualizes a biological pathway with a high impact in tumor treatment. Therefore, it could play an important role in the development of new image-based dose distributions and guide treatment fractionation strategies and deserves to be investigated in future clinical trials.

9.3.3 Angiogenesis

The αvβ3 integrin is an important receptor for cell adhesion involved in tumor-induced angiogenesis and metastasis. It mediates migration of activated endothelial cells through the basement membrane during formation of new blood vessels. Particularly interesting is that this integrin is expressed only on the cell surface of tumor cells or activated endothelial cells, and not on normal endothelial cells of established vessels. Haubner et al. (2001) and Beer et al. (2007) described the noninvasive imaging of αvβ3 integrin expression using F18-labeled RDG-containing glycopeptide and PET. In squamous cell carcinoma of head and neck, for example, αvβ3 integrin seems to be expressed on the endothelial cells and not on the tumor cells. This suggests that RGD-PET could be used as a surrogate for the visualization and evaluation of tumor angiogenesis (Beer et al. 2007).

9.4 Conclusion

PET could improve the delineation of GTV in some tumor entities like brain tumors, lung cancer, and head and neck cancer. Therefore, its impact on the clinical outcome has to be evaluated in prospective trials. The role of PET for the visualization of tumor biology is unclear. However, this approach could open new perspectives in treatment planning and monitoring of solid tumors and has to be assessed in the future in experimental and clinical studies.

References

Abouzied MM, Crawford ES, Nabi HA (2005) 18F-FDG imaging: pitfalls and artifacts. J Nucl Med Technol 33:145–155

Alber M, Paulsen F, Eschmann SM, Machulla HJ (2003) On biologically conformal boost dose optimization. Phys Med Biol 48:N31–N35

Beer AJ, Grosu AL, Carlsen J, Kolk A, Sabria M, Stangier I, Watzlowik P, Wester HJ, Haubner R, Schwaiger M (2007) Feasibility of (18F)galacto-RGD PET for imaging of αvβ3 expression on neovasculature in patients with squamous cell carcinoma of head and neck. Clin Cancer Res 13:6610–6616

Bentzen SM (2005) Radiation therapy: intensity modulated, image guided, biologically optimized and evidence based. Radiother Oncol 77:227–230

Bradley J, Thorstad WL, Mutic S, Miller TR, Dehdashti F, Siegel BA, Bosch W, Bertrand RJ (2004) Impact of FDG-PET on radiation therapy volume delineation in non-small-cell lung cancer. Int J Radiat Oncol Biol Phys 59:78–86

Buck AK, Hetzel M, Schirrmeister H, Halter G, Moller P, Kratochwil C, Wahl A, Glatting G, Mottaghy FM, Mattfeldt T, Neumaier B, Reske SN (2005) Clinical relevance of imaging proliferative activity in lung nodules. Eur J Nucl Med Mol Imaging 32:525–533

Bussink J, Kaanders JH, van der Kogel AJ (2003) Tumor hypoxia at the micro-regional level: clinical relevance and predictive value of exogenous and endogenous hypoxic cell markers. Radiother Oncol 67:3–15

Caldwell CB, Mah K, Ung YC, Danjoux CE, Balogh JM, Ganguli SN, Ehrlich LE (2001) Observer variation in contouring gross tumor volume in patients with poorly defined non-small-cell lung tumors on CT: the impact of 18FDG-hybrid PET fusion. Int J Radiat Oncol Biol Phys 51:923–931

Caldwell CB, Mah K, Skinner M, Danjoux CE (2003) Can PET provide the 3D extent of tumor motion for individualized internal target volumes? A phantom study of the limitations of CT and the promise of PET. Int J Radiat Oncol Biol Phys 55:1381–1393

Chan SC, Ng SH, Chang JT, Lin CY, Chen YC, Chang YC, Hsu CL, Wang HM, Liao CT, Yen TC (2006) Advantages and pitfalls of 18F-fluoro-2-deoxy-D-glucose positron emission tomography in detecting locally residual or recurrent nasopharyngeal carcinoma: comparison with magnetic resonance imaging. Eur J Nucl Med Mol Imaging 33:1032–1040

Chao KS, Bosch WR, Mutic S, Lewis JS, Dehdashti F, Mintun MA, Dempsey JF, Perez CA, Purdy JA, Welch MJ (2001) A novel approach to overcome hypoxic tumor resistance: Cu-ATSM-guided intensity-modulated radiation therapy. Int J Radiat Oncol Biol Phys 49:1171–1182

Cherry SR (2006) The 2006 Henry N. Wagner Lecture: Of mice and men (and positrons)–advances in PET imaging technology. J Nucl Med 47:1735–1745

Ciernik IF, Dizendorf E, Baumert BG, Reiner B, Burger C, Davis JB, Lutolf UM, Steinert HC, Von Schulthess GK (2003) Radiation treatment planning with an integrated positron emission and computer tomography (PET/CT): a feasibility study. Int J Radiat Oncol Biol Phys 57:853–863

Connell CA, Corry J, Milner AD, Hogg A, Hicks RJ, Rischin D, Peters LJ (2007) Clinical impact of, and prognostic stratification by, F-18 FDG PET/CT in head and neck mucosal squamous cell carcinoma Head Neck 29:986–995

Daisne JF, Sibomana M, Bol A, Doumont T, Lonneux M, Gregoire V (2003) Tri-dimensional automatic segmentation of PET volumes based on measured source-to-background ratios: influence of reconstruction algorithms. Radiother Oncol 69:247–250

Daisne JF, Duprez T, Weynand B, Lonneux M, Hamoir M, Reychler H, Gregoire V (2004) Tumor volume in pharyngolaryngeal squamous cell carcinoma: comparison of CT, MR imaging, and FDG PET and validation with surgical specimen. Radiology 233:93–100

Dehdashti F, Mintun MA, Lewis JS, Bradley J, Govindan R, Laforest R, Welch MJ, Siegel BA (2003) In vivo assessment of tumor hypoxia in lung cancer with 60Cu-ATSM. Eur J Nucl Med Mol Imaging 30:844–850

De Ruysscher D, Wanders S, van Haren E, Hochstenbag M, Geeraedts W, Utama I, Simons J, Dohmen J, Rhami A, Buell U, Thimister P, Snoep G, Boersma L, Verschueren T, van Baardwijk A, Minken A, Bentzen SM, Lambin P (2005) Selective mediastinal node irradiation based on FDG-PET scan data in patients with non-small-cell lung cancer: a prospective clinical study. Int J Radiat Oncol Biol Phys 62:988–994

Dresel S, Grammerstorff J, Schwenzer K, Brinkbaumer K, Schmid R, Pfluger T, Hahn K (2003) [18F]FDG imaging of head and neck tumours: comparison of hybrid PET and morphological methods. Eur J Nucl Med Mol Imaging 30:995–1003

Dwamena BA, Sonnad SS, Angobaldo JO, Wahl RL (1999) Metastases from non-small cell lung cancer: mediastinal staging in the 1990s–meta-analytic comparison of PET and CT. Radiology 213:530–536

Erdi YE, Mawlawi O, Larson SM, Imbriaco M, Yeung H, Finn R, Humm JL (1997) Segmentation of lung lesion volume by adaptive positron emission tomography image thresholding. Cancer 80:2505–2509

Eschmann SM, Paulsen F, Reimold M, Dittmann H, Welz S, Reischl G, Machulla HJ, Bares R (2005) Prognostic impact of hypoxia imaging with 18F-misonidazole PET in non-small cell lung cancer and head and neck cancer before radiotherapy. J Nucl Med 46:253–260

Ford EC, Kinahan PE, Hanlon L, Alessio A, Rajendran J, Schwartz DL, Phillips M (2006) Tumor delineation using PET in head and neck cancers: threshold contouring and lesion volumes. Med Phys 33:4280–4288

Gambhir SS, Czernin J, Schwimmer J, Silverman DH, Coleman RE, Phelps ME (2001) A tabulated summary of the FDG PET literature. J Nucl Med 42:1S–93S

Geets X, Lee JA, Bol A, Lonneux M, Gregoire V (2007) A gradient-based method for segmenting FDG-PET images: methodology and validation. Eur J Nucl Med Mol Imaging 34:1427–1438

Goshen E, Davidson T, Yahalom R, Talmi YP, Zwas ST (2006) PET/CT in the evaluation of patients with squamous cell cancer of the head and neck. Int J Oral Maxillofac Surg 35:332–336

Grosu AL, Weber W, Feldmann HJ, Wuttke B, Bartenstein P, Gross MW, Lumenta C, Schwaiger M, Molls M (2000) First experience with I-123-alpha-methyl-tyrosine SPECT in the 3-D radiation treatment planning of brain gliomas. Int J Radiat Oncol Biol Phys 47:517–526

Grosu AL, Feldmann H, Dick S, Dzewas B, Nieder C, Gumprecht H, Frank A, Schwaiger M, Molls M, Weber WA (2002) Implications of IMT-SPECT for postoperative radiotherapy planning in patients with gliomas. Int J Radiat Oncol Biol Phys 54:842–854

Grosu AL, Lachner R, Wiedenmann N, Stark S, Thamm R, Kneschaurek P, Schwaiger M, Molls M, Weber WA (2003) Validation of a method for automatic image fusion (BrainLAB System) of CT data and 11C-methionine-PET data for stereotactic radiotherapy using a LINAC: first clinical experience. Int J Radiat Oncol Biol Phys 56:1450–1463

Grosu AL, Weber WA, Riedel E, Jeremic B, Nieder C, Franz M, Gumprecht H, Jaeger R, Schwaiger M, Molls M (2005a) L-(methyl-11C) methionine positron emission tomography for target delineation in resected high-grade gliomas before radiotherapy Int J Radiat Oncol Biol Phys 63:64–74

Grosu AL, Weber WA, Franz M, Stark S, Piert M, Thamm R, Gumprecht H, Schwaiger M, Molls M, Nieder C (2005b) Reirradiation of recurrent high-grade gliomas using amino acid PET (SPECT)/CT/MRI image fusion to determine gross tumor volume for stereotactic fractionated radiotherapy. Int J Radiat Oncol Biol Phys 63:511–519

Grosu AL, Piert M, Molls M (2005c) Experience of PET for target localisation in radiation oncology. Br J Radiol 78:18–32

Grosu AL, Souvatzoglou M, Roper B, Dobritz M, Wiedenmann N, Jacob V, Wester HJ, Reischl G, Machulla HJ, Schwaiger M, Molls M, Piert M (2007) Hypoxia imaging with FAZA-PET and theoretical considerations with regard to dose painting for individualization of radiotherapy in patients with head and neck cancer. Int J Radiat Oncol Biol Phys 69:541–551

Haubner R, Wester HJ, Weber WA (2001) Noninvasive imaging of alpha(v)beta3 integrin expression using 18F-labeled RGD-containing glycopeptide and positron emission tomography Cancer Res 61:1781–1785

Hellwig D, Ukena D, Paulsen F, Bamberg M, Kirsch CM (2001) Meta-analysis of the efficacy of positron emission tomography with F-18-fluorodeoxyglucose in lung tumors. Basis for discussion of the German Consensus Conference on PET in Oncology 2000. Pneumologie 55:367–377

Ireland RH, Dyker KE, Barber DC, Wood SM, Hanney MB, Tindale WB, Woodhouse N, Hoggard N, Conway J, Robinson MH (2007) Nonrigid image registration for head and neck cancer radiotherapy treatment planning with PET/CT. Int J Radiat Oncol Biol Phys 68:952–957

Jeong HJ, Min JJ, Park JM, Chung JK, Kim BT, Jeong JM, Lee DS, Lee MC, Han SK, Shim YS (2002) Determination of the prognostic value of [^{18}F]fluorodeoxyglucose uptake by using positron emission tomography in patients with non-small cell lung cancer. Nucl Med Commun 23:865–870

Kiricuta IC (2001) Selection and delineation of lymph node target volume for lung cancer conformal radiotherapy. Proposal for standardizing terminology based on surgical experience. Strahlenther Onkol 177:410–423

Koh WJ, Bergman KS, Rasey JS, Peterson LM, Evans ML, Graham MM, Grierson JR, Lindsley KL, Lewellen TK, Krohn KA (1995) Evaluation of oxygenation status during fractionated radiotherapy in human non-small cell lung cancers using [F-18]fluoromisonidazole positron emission tomography. Int J Radiat Oncol Biol Phys 33:391–398

Koritzinsky M, Seigneuric R, Magagnin MG, van den Beucken T, Lambin P, Wouters BG (2005) The hypoxic proteome is influenced by gene-specific changes in mRNA translation. Radiother Oncol 76:177–186

Langen KJ, Ziemons K, Kiwit JC, Herzog H, Kuwert T, Bock WJ, Stocklin G, Feinendegen LE, Muller-Gartner HW (1997) 3-[123I]iodo-alpha-methyltyrosine and [methyl-11C]-L-methionine uptake in cerebral gliomas: a comparative study using SPECT and PET. J Nucl Med 38:517–522

Lee NY, Mechalakos JG, Nehmeh S, Lin Z, Squire OD, Cai S, Chan K, Zanzonico PB, Greco C, Ling CC, Humm JL, Schöder H (2008) Fluorine-18-labeled fluoromisonidazole positron emission and computed tomography-guided intensity-modulated radiotherapy for head and neck cancer: a feasibility study. Int J Radiat Oncol Biol Phys 70:2–13

Ling CC, Humm J, Larson S, Amols H, Fuks Z, Leibel S, Koutcher JA (2000) Towards multidimensional radiotherapy (MD-CRT): biological imaging and biological conformality. Int J Radiat Oncol Biol Phys 47:551–560

Ling CC, Yorke E, Amols H, Mechalakos J, Erdi Y, Leibel S, Rosenzweig K, Jackson A (2004) High-tech will improve radiotherapy of NSCLC: a hypothesis waiting to be validated. Int J Radiat Oncol Biol Phys 60:3–7

Liu T, Xu W, Yan WL, Ye M, Bai YR, Huang G (2007) FDG-PET, CT, MRI for diagnosis of local residual or recurrent nasopharyngeal carcinoma, which one is the best? A systematic review. Radiother Oncol 85:327–335

MacManus MP, Hicks RJ, Matthews JP, Hogg A, McKenzie AF, Wirth A, Ware RE, Ball DL (2001) High rate of detection of unsuspected distant metastases by PET in apparent stage III non-small-cell lung cancer: implications for radical radiation therapy. Int J Radiat Oncol Biol Phys 50:287–293

MacManus MP, Bayne M, Fimmell N, Reynolds J, Everitt S, Ball D, Pitman A, Ware R, Lau E (2007) Reproducibility of "intelligent" contouring of gross tumor volume in non-small cell lung cancer on PET/CT images using a standardized visual method. Int J Radiat Oncol Biol Phys 69:S154–S155

Madani I, Duthoy W, Derie C, De Gersem W, Boterberg T, Saerens M, Jacobs F, Gregoire V, Lonneux M, Vakaet L, Vanderstraeten B, Bauters W, Bonte K, Thierens H, De Neve W (2007) Positron emission tomography-guided, focal-dose escalation using intensity-modulated radiotherapy for head and neck cancer. Int J Radiat Oncol Biol Phys 68:126–135

Munley MT, Marks LB, Scarfone C, Sibley GS, Patz EF Jr, Turkington TG, Jaszczak RJ, Gilland DR, Anscher MS, Coleman RE (1999) Multimodality nuclear medicine imaging in three-dimensional radiation treatment planning for lung cancer: challenges and prospects. Lung Cancer 23:105–114

Nakamoto Y, Tatsumi M, Hammoud D, Cohade C, Osman MM, Wahl RL (2005) Normal FDG distribution patterns in the head and neck: PET/CT evaluation. Radiology 234:879–885

Nehmeh SA, Lee NY, Schroder H, Squire O, Zanzonico PB, Erdi YE, Greco C, Mageras G, Pham HS, Larson SM, Ling CC, Humm JL (2008) Reproducibility of intratumor distribution of (18)F-fluoromisonidazole in head and neck cancer. Int J Radiat Oncol Biol Phys 70:235–242

Nestle U, Walter K, Schmidt S, Licht N, Nieder C, Motaref B, Hellwig D, Niewald M, Ukena D, Kirsch CM, Sybrecht GW, Schnabel K (1999) 18F-deoxyglucose positron emission tomography (FDG-PET) for the planning of radiotherapy in lung cancer: high impact in patients with atelectasis. Int J Radiat Oncol Biol Phys 44:593–597

Nestle U, Hellwig D, Schmidt S, Licht N, Walter K, Ukena D, Rübe C, Baumann M, Kirsch CM (2002) 2-Deoxy-2-[18F] fluoro-D-glucose positron emission tomography in target volume definition for radiotherapy of patients with non-small-cell lung cancer. Mol Imaging Biol 4:257–263

Nestle U, Kremp S, Schaefer-Schuler A, Sebastian-Welsch C, Hellwig D, Rübe C, Kirsch CM (2005) Comparison of different methods for delineation of 18F-FDG PET-positive tissue for target volume definition in radiotherapy of patients with non-small cell lung cancer. J Nucl Med 46:1342–1348

Nestle U, Kremp S, Grosu A (2006) Practical integration of [(18)F]-FDG-PET and PET-CT in the planning of radiotherapy for non-small cell lung cancer (NSCLC): the technical basis, ICRU-target volumes, problems, perspectives. Radiother Oncol 81:209–225

Nestle U, Schaefer-Schuler A, Kremp S, Groeschel A, Hellwig D, Rube C, Kirsch CM (2007) Target volume definition for (18)F-FDG PET-positive lymph nodes in radiotherapy of patients with non-small cell lung cancer. Eur J Nucl Med Mol Imaging 34:453–462

Nishioka T, Shiga T, Shirato H, Tsukamoto E, Tsuchiya K, Kato T, Ohmori K, Yamazaki A, Aoyama H, Hashimoto S, Chang TC, Miyasaka K (2002) Image fusion between 18FDG-PET and MRI/CT for radiotherapy planning of oropharyngeal and nasopharyngeal carcinomas. Int J Radiat Oncol Biol Phys 53:1051–1057

Nordsmark M, Bentzen SM, Rudat V, Brizel D, Lartigau E, Stadler P, Becker A, Adam M, Molls M, Dunst J, Terris DJ, Overgaard J (2005) Prognostic value of tumor oxygenation in 397 head and neck tumors after primary radiation therapy. An international multi-center study. Radiother Oncol 77:18–24

Paulino AC, Koshy M, Howell R, Schuster D, Davis LW (2005) Comparison of CT- and FDG-PET-defined gross tumor volume in intensity-modulated radiotherapy for head-and-neck cancer. Int J Radiat Oncol Biol Phys 61:1385–1392

Pötzsch C, Hofheinz F, van den Hoff J (2006) Vergleich der Inter-Observer-Variabilität bei manueller und automatischer Volumenbestimmung in der PET. Nuklearmedizin (German) 45:A42

Rahn AN, Baum RP, Adamietz IA, Adams S, Sengupta S, Mose S, Bormeth SB, Hor G, Bottcher HD (1998) Value of 18F fluorodeoxyglucose positron emission tomography in radiotherapy planning of head-neck tumors. Strahlenther Onkol 174:358–364

Rasey JS, Koh WJ, Evans ML, Peterson LM, Lewellen TK, Graham MM, Krohn KA (1996) Quantifying regional hypoxia in human tumors with positron emission tomography of [18F]fluoromisonidazole: a pretherapy study of 37 patients. Int J Radiat Oncol Biol Phys 36:417–428

Rosenzweig KE, Sura S, Jackson A, Yorke E (2007) Involved-field radiation therapy for inoperable non-small-cell lung cancer. J Clin Oncol 25:5557–5561

Scarfone C, Lavely WC, Cmelak AJ, Delbeke D, Martin WH, Billheimer D, Hallahan DE (2004) Prospective feasibility trial of radiotherapy target definition for head and neck cancer using 3-dimensional PET and CT imaging J Nucl Med 45:543–552

Schaefer A, Kremp S, Hellwig D, Ruebe C, Kirsch CM, Nestle U (2008) A contrast-oriented algorithm for FDG-PET-based delineation of tumour volumes for the radiotherapy of lung cancer: derivation from phantom measurements and validation in patient data. Eur J Nucl Med Mol Imaging 35: 1989–1999

Schinagl DA, Vogel WV, Hoffmann AL, van Dalen JA, Oyen WJ, Kaanders JH (2007) Comparison of five segmentation tools for 18F-fluoro-deoxy-glucose-positron emission tomography-based target volume definition in head and neck cancer. Int J Radiat Oncol Biol Phys 69:1282–1289

Schöder H, Carlson DL, Kraus DH, Stambuk HE, Gonen M, Erdi YE, Yeung HW, Huvos AG, Shah JP, Larson SM, Wong RJ (2006) 18F-FDG PET/CT for detecting nodal metastases in patients with oral cancer staged N0 by clinical examination and CT/MRI. J Nucl Med 47:755–762

Schwartz DL, Ford E, Rajendran J, Yueh B, Coltrera MD, Virgin J, Anzai Y, Haynor D, Lewellyn B, Mattes D, Meyer J, Phillips M, Leblanc M, Kinahan P, Krohn K, Eary J, Laramore GE (2005a) FDG-PET/CT imaging for preradiotherapy staging of head-and-neck squamous cell carcinoma. Int J Radiat Oncol Biol Phys 61:129–136

Schwartz DL, Ford EC, Rajendran J, Yueh B, Coltrera MD, Virgin J, Anzai Y, Haynor D, Lewellen B, Mattes D, Kinahan P, Meyer J, Phillips M, Leblanc M, Krohn K, Eary J, Laramore GE (2005b) FDG-PET/CT-guided intensity modulated head and neck radiotherapy: a pilot investigation. Head Neck 27:478–487

Shields AF, Grierson JR, Dohmen BM, Machulla HJ, Stayanoff JC, Lawhorn-Crews JM, Obradovich JE, Muzik O, Mangner TJ (1998) Imaging proliferation in vivo with [F-18]FLT and positron emission tomography. Nat Med 4:1334–1336

Steenbakkers RJ, Duppen JC, Fitton I, Deurloo KE, Zijp LJ, Comans EF, Uitterhoeve AL, Rodrigus PT, Kramer GW, Bussink J, De Jaeger K, Belderbos JS, Nowak PJ, van Herk M, Rasch CR (2006) Reduction of observer variation using matched CT-PET for lung cancer delineation: a three-dimensional analysis. Int J Radiat Oncol Biol Phys 64:435–448

Sura S, Greco C, Gelblum D, Yorke ED, Jackson A, Rosenzweig KE (2008) (18)F-fluorodeoxyglucose positron emission tomography-based assessment of local failure patterns in non-small-cell lung cancer treated with definitive radiotherapy. Int J Radiat Oncol Biol Phys 70:1397–1402

Tanderup K, Olsen DR, Grau C (2006) Dose painting: art or science? Radiother Oncol 79:245–248

Troost EG, Bussink J, Kaanders JH, van Eerd J, Peters JP, Rijken PF, Boerman OC, van der Kogel AJ (2005) Comparison of different methods of CAIX quantification in relation to hypoxia in three human head and neck tumor lines. Radiother Oncol 76:194–199

Van de Steene J, Linthout N, de Mey J, Vinh-Hung V, Claassens C, Noppen M, Bel A, Storme G (2002) Definition of gross tumor volume in lung cancer: inter-observer variability. Radiother Oncol 62:37–49

Weber WA, Wester HJ, Grosu AL, Herz M, Dzewas B, Feldmann HJ, Molls M, Stocklin G, Schwaiger M (2000) O-(2-[18F]fluoroethyl)-L-tyrosine and L-[methyl-11C] methionine uptake in brain tumours: initial results of a comparative study. Eur J Nucl Med 27:542–549

Weber WA, Dick S, Reidl G, Dzewas B, Busch R, Feldmann HJ, Molls M, Lumenta CB, Schwaiger M, Grosu AL (2001) Correlation between postoperative 3-[(123)I]iodo-L-alpha-methyltyrosine uptake and survival in patients with gliomas. J Nucl Med 42:1144–1150

Weber WA, Grosu AL, Czernin J (2008) Technology insight: advances in molecular imaging and an appraisal of PET/CT scanning. Nat Clin Pract Oncol 5:160–170

Williams KJ, Telfer BA, Xenaki D, Sheridan MR, Desbaillets I, Peters HJ, Honess D, Harris AL, Dachs GU, van der Kogel A, Stratford IJ (2005) Enhanced response to radiotherapy in tumours deficient in the function of hypoxia-inducible factor-1. Radiother Oncol 75:89–98

Yap CS, Czernin J, Fishbein MC, Cameron RB, Schiepers C, Phelps ME, Weber WA (2006) Evaluation of thoracic tumors with 18F-fluorothymidine and 18F-fluorodeoxyglucose-positron emission tomography Chest 129:393–401

Yaremko B, Riauka T, Robinson D, Murray B, Alexander A, McEwan A, Roa W (2005) Thresholding in PET images of static and moving targets. Phys Med Biol 50:5969–5982

Yaromina A, Holscher T, Eicheler W, Rosner A, Krause M, Hessel F, Petersen C, Thames HD, Baumann M, Zips D (2005) Does heterogeneity of pimonidazole labelling correspond to the heterogeneity of radiation-response of FaDu human squamous cell carcinoma? Radiother Oncol 76:206–212

Zimny M, Wildberger JE, Cremerius U, DiMartino E, Jaenicke S, Nowak B, Bull U (2002) Combined image interpretation of computed tomography and hybrid PET in head and neck cancer. Nuklearmedizin 41:14–21